CSIRO PUBLISHING

Australian Journal of Physics

Volume 52, 1999

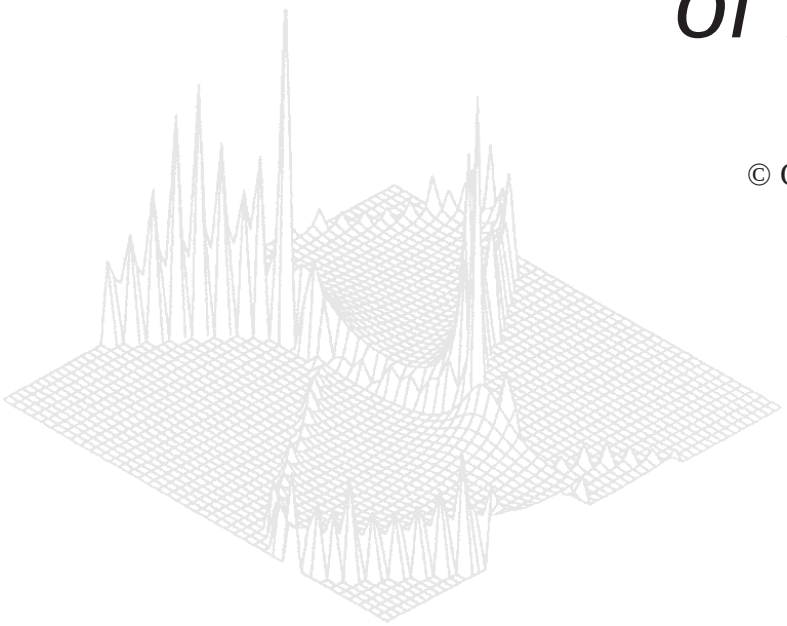

A journal for the publication of
original research in all branches of physics

www.publish.csiro.au/journals/ajp

All enquiries and manuscripts should be directed to
Australian Journal of Physics
CSIRO PUBLISHING
PO Box 1139 (150 Oxford St)
Collingwood Telephone: 61 3 9662 7626
Vic. 3066 Facsimile: 61 3 9662 7611
Australia Email: peter.robertson@publish.csiro.au

Published by **CSIRO** PUBLISHING
for CSIRO Australia and
the Australian Academy of Science

Aust. J. Phys., 1999, **52**, 537–44

Angular Distribution of Hydrogen Fragment Ions in H^+–H_2 Collisions*

Bärbel Siegmann and Rainer Hippler[A]

Fakultät für Physik, Universität Bielefeld,
Postfach 100 131, 33501 Bielefeld, Germany.
[A]Present address: Institut für Physik,
Ernst-Moritz-Arndt-Universität Greifswald,
Domstraße 10a, 17487 Greifswald, Germany.

Abstract

The angular distribution of H^+ fragment ions produced in 5–25 keV H^+–H_2 collisions was investigated in coincidence with Lyman-α photons. The observed photons arise from electron capture to the projectile H(2p) state and/or from the fragmentation of the H_2 molecule via $2s\sigma_g$, $2p\sigma_u$ or $2p\pi_u$ states of the excited H_2^{+*} ion. An analysis of the measured angular distributions has been performed to distinguish the separate degenerate channels available to an emitted Lyman-α photon. The results show similarities to the data of Lindsay *et al.* (1987) who measured the non-coincident angular distribution of H^+ fragment ions within the same energy range.

1. Introduction

Dissociative ionisation by electrons and photons has been extensively studied by several groups (Dunn and Kiefer 1963; Crowe and McConkey 1973; Dehmer and Dill 1978; Lindsay *et al.* 1987). The measured energy and angular distributions of the product ions showed that the structures of the spectra can be explained by excitation to several repulsive states of the excited H_2^{+*} ion formed during the collision. From the energy distribution of the fragment ions it was possible to identify different dissociation processes. Additionally, angular distribution measurements provided information on the symmetry of the repulsive states.

At the centre of our attention is the H^+–H_2 system as a prototype case for the study of two electron processes during collisions involving molecules. For this system we performed an experiment in which a Lyman-α photon (wavelength $\lambda = 121{\cdot}6$ nm) is detected in coincidence with a H^+ fragment ion from the dissociating H_2 molecule, and where the Lyman-α photon results from the decay of an excited H($2p$) atom into its H($1s$) ground state. The only other experiment to compare our results with was performed by Lindsay *et al.* (1987) who investigated the non-coincident energy and angular distribution of fragment ions.

The processes in question for the present experiment are charge exchange excitation to the H($2p$) state of the projectile and the simultaneous formation of an intermediate $H_2^{+*}(2p\sigma_u)$ state,

* Refereed paper based on a contribution to the Australia–Germany Workshop on Electron Correlations held in Fremantle, Western Australia, on 1–6 October 1998.

 10.1071/PH99021 0004-9506/99/030537$05.00

$$H^+ + H_2 \longrightarrow H(2p) + H_2^{+*}\,, \tag{1}$$

where the excited $H_2^{+*}(2s\sigma_g)$, $H_2^{+*}(2p\sigma_u)$ and $H_2^{+*}(2p\pi_u)$ states accessed in the present experiment either decay via

$$H_2^{+*}(2p\sigma_u) \rightarrow H^+ + H(1s) \tag{2}$$

into a H^+ fragment ion and a neutral $H(1s)$ atom in its ground state, or via

$$H_2^{+*}(2s\sigma_u, 2p\pi_u) \rightarrow H^+ + H(n=2) \tag{3}$$

into a H^+ fragment ion and an excited H atom either in the $H(2s)$ or the $H(2p)$ state. During the fragmentation process internal energy is converted into kinetic energy which is equally shared by the two fragments. This fragmentation energy will depend on the intermediate H_2^{+*} state formed in the collision; for the above processes this kinetic energy is in the 5–10 eV range (Table 1). The formation of excited $H_2^{+*}(2s\sigma_g, 2p\pi_u)$ states itself may give rise to the emission of a Lyman-α photon via the decay into a $H(2p)$ state (equation 3); in this case we cannot distinguish between the charge exchange process

$$H^+ + H_2 \longrightarrow H(nl) + H_2^{+*}(2s\sigma_u, 2p\pi_u) \tag{4}$$

and the direct ionisation process

$$H^+ + H_2 \longrightarrow H^+ + H_2^{+*}(2s\sigma_u, 2p\pi_u) + e^-\,. \tag{5}$$

To distinguish between processes (4) and (5) a triple coincidence employing a charge state analysis of the final projectile state is required which has not yet been performed.

Finally, the H_2 molecule may become completely ionised during the collision. The process which we have investigated with our Lyman-α photon fragment ion coincidence technique is

$$H^+ + H_2 \longrightarrow H(2p) + H^+ + H^+ + e^-\,. \tag{6}$$

To separate the different molecular excitation processes from each other we made use of the different kinetic energies (Table 1) received by the H^+ ions during dissociation which result in different time-of-flights to the ion detector. The incident energy was in the range 5–25 keV.

2. Experimental Set-up

A proton beam with kinetic energies of 5–25 keV was produced in a duoplasmatron ion source (Hippler *et al.* 1988). After mass separation the collimated projectile beam interacts with a molecular hydrogen target gas. In order to separate the different excitation channels the emitted Lyman-α radiation is detected in coincidence with a H^+ fragment ion. The Lyman-α photon is registered in a photomultiplier and serves as a start pulse for the coincidence unit. The positive ions are extracted by a weak electric field (25 V/cm) perpendicular to the direction

of the incident ion beam. After passing a field-free time-of-flight region they are accelerated a second time to enhance the detector efficiency of the position- and time-sensitive detector. The ion detector consists of micro-channel plates in a chevron configuration in combination with a multi-segment anode.

Table 1. Kinetic energy of fragment ion and asymmetry parameter β for the dissociative ionisation of H_2^+ (after Lindsay *et al.* 1987)

Molecular state of H_2^+	Energy of H^+	Symmetry e^-	Symmetry of $H_2^+ + e^-$	β parameter
$2p\pi_u$	5·0 eV	σ_g	Π_u	–1
		π_g	Σ_u	+2
		δ_g	Π_u	–1
$2s\sigma_g$	5·8 eV	σ_u	Σ_u	+2
		π_u	Π_u	–1
$2p\sigma_u$	7·9 eV	σ_g	Σ_u	+2
		π_g	Π_u	–1
H^+H^+	9·5 eV			0

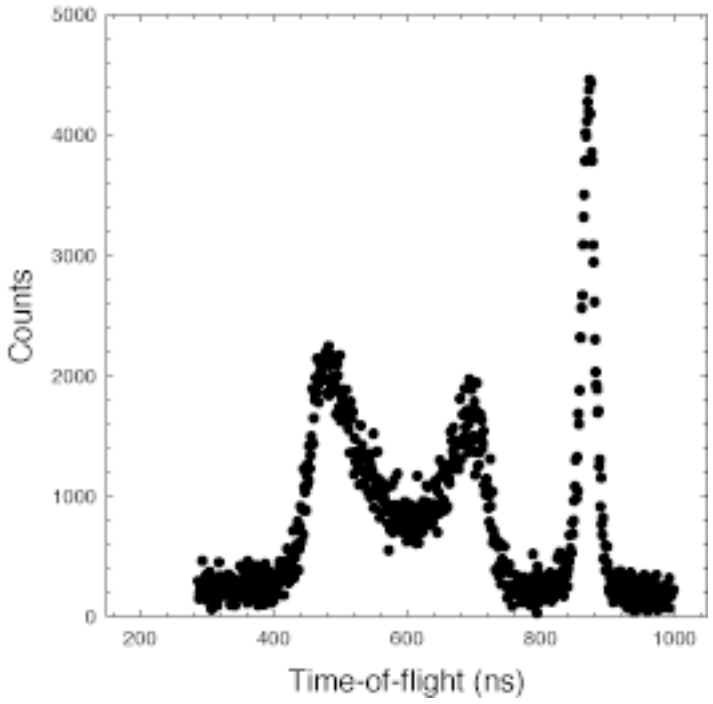

Fig. 1. Time-of-flight spectrum of H^+ ions in coincidence with Lyman-α photons (see text). A constant background was subtracted from the data. The two broad peaks around 500 ns and 700 ns arise from H^+ fragment ions ejected in forward and backward directions, respectively, with respect to the ion detector; the narrow peak around 900 ns arises from H_2^+ molecular ions.

The central part of the coincidence electronics is a 32-channel multi-hit *time-to-digital converter* with a time-resolution of better than 1 ns. The system is started by a Lyman-α photon registered in the photomultiplier; it is stopped by an ion pulse from the anode of the micro-channel-plate detector. Fig. 1 shows a typical time-of-flight spectrum of fragment ions. The two peaks correspond to H^+ ions emitted at forward and backward angles, respectively, with respect to the ion detector. From the coincidence measurement the time-of-flight and the position of the fragment ions upon arrival at the ion detector are extracted, which in turn are related to the emission angle and the kinetic energy of the fragment ion. These quantities serve to identify the different processes.

In the data analysis the energy distribution of the H^+ fragments (Fig. 1) was simulated using the reflection approximation. The ground state wavefunction was calculated using the Numerov technique (Yousif *et al*. 1988). A fit with the *maximum-entropy method* to the experimental data was used to extract the cross section for each emission angle. With an electric field of 25 V/cm an estimated energy resolution of $0{\cdot}4$ eV was achieved. However, due to relatively low counting statistics in the present coincidence experiment and since each peak is ≈ 2 eV wide, it was not possible to separate the $H_2^{+*}(2s\sigma_g)$ from the $H_2^{+*}(2p\pi_u)$ intermediate state; these states have, hence, been analysed together.

Dehmer and Dill (1978) have shown that in photoionisation the angular distribution of the fragment ion is given by

$$\frac{d\sigma}{d\Omega} = \frac{\sigma_{\mathrm{tot}}}{4\pi}\Big(1 + \beta P_2(\cos\theta)\Big)\,, \tag{7}$$

where σ_{tot} is the total cross section, $P_2(\cos\theta) = \frac{1}{2}(3\cos^2\theta - 1)$ is the second Legendre polynomial, and θ is the angle between the molecular axis at the instant of the collision and the z-axis which in the present case coincides with the direction of the incident projectile. Here β is the asymmetry parameter which can vary between $\beta = -1$ and $\beta = +2$. Equation (7) was derived under the assumption of dipole transitions which is the case in photoionisation. The extent to which this equation holds for particle impact ionisation is not yet clear. As we shall see below, however, equation (7) nevertheless provides a useful parametrisation of the measured angular distribution for the atomic collision process reported here.

Since the excited states of diatomic molecules are degenerate with respect to the magnetic quantum number $|M_l|$, the symmetry of the excited H_2^{+*} molecular ions can, for a dipole-allowed transition, be either σ_g, σ_u or π_u. A transition with $\Delta M_l = 0$ yields $\beta = -1$ resulting in a $\sin^2\theta$ distribution; a $\Delta M_l = \pm 1$ transition yields $\beta = +2$ and a $\cos^2\theta$ distribution. Table 1 shows the possible fragmentation channels for the dissociation of H_2 and the corresponding theoretical β parameter.

The angular distribution of H^+ fragment ions from $H_2^{+*}(2p\sigma_u)$ and $H_2^{+*}(2s\sigma_g, 2p\pi_u)$ measured at 15 keV in coincidence with Lyman-α photons is displayed in Fig. 2. The dashed lines are corresponding fits according to equation (7). The different symmetry of the two data sets resulting in different β parameters is obvious.

Most of the time the measured asymmetry parameter β is a mixture of two or more degenerate channels. In the cases considered here, only $\Sigma \rightarrow \Sigma$ and $\Sigma \rightarrow \Pi$ transitions are possible. The ratio of these cross sections for these transitions

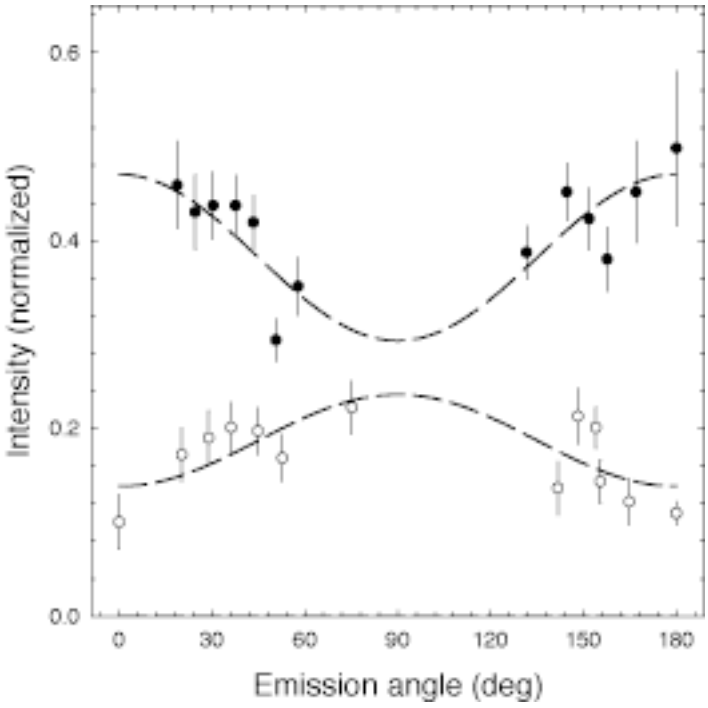

Fig. 2. Angular distributions of H^+ fragment ions from the decay of (•) ${H_2}^{+*}(2p\sigma_u)$ and (○) ${H_2}^{+*}(2s\sigma_g, 2p\pi_u)$ molecules. The incident energy was 15 keV. Dashed lines are corresponding fits according to equation (7).

can be determined from the measured β (Dehmer and Dill 1978; Lindsay *et al.* 1987):

$$\frac{\sigma(\Sigma \to \Sigma)}{\sigma(\Sigma \to \Pi)} = \frac{1+\beta}{4-2\beta}\,. \tag{8}$$

In the following we apply this concept to the ionisation of H_2 by ion impact which may be justified as long as the interaction is Coulombic in nature and dominated by optically allowed transitions.

3. Results and Discussion

The asymmetry parameter β for the $H_2^{+*}(2p\sigma_u)$ channel (equation 1) as a function of projectile energy is displayed in Fig. 3. The measured β is positive and close to $+1{\cdot}5$ at low incident energies; it approaches zero around 20 keV. With the exception of the data point at 5 keV our results are in fair agreement with the asymmetry parameter β as measured by Lindsay *et al.* It should be emphasised that Lindsay *et al.* (1987) used a non-coincidence technique which did not distinguish between the direct ionisation process

$$H^+ + H_2 \longrightarrow H^+ + H_2^{+*}(2p\sigma_u) + e^- \tag{9}$$

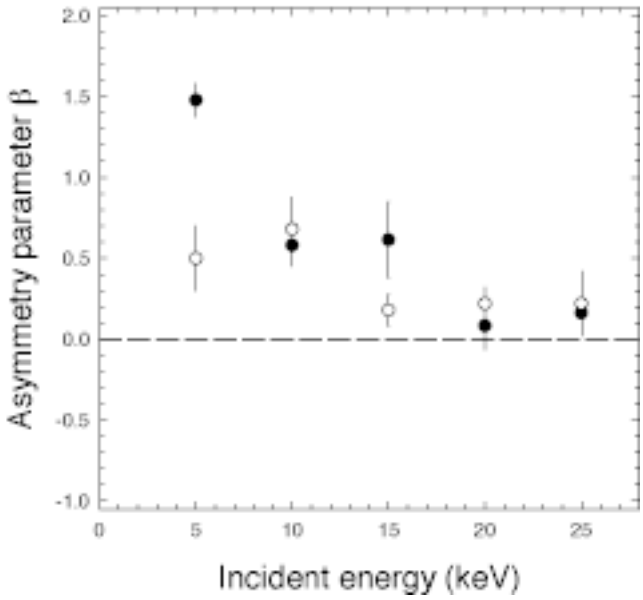

Fig. 3. Asymmetry parameter β versus incident energy for the decay of the $H_2^{+*}(2p\sigma_u)$ molecule in H^+–H_2 collisions: •, present results; ○ Lindsay *et al.* (1987).

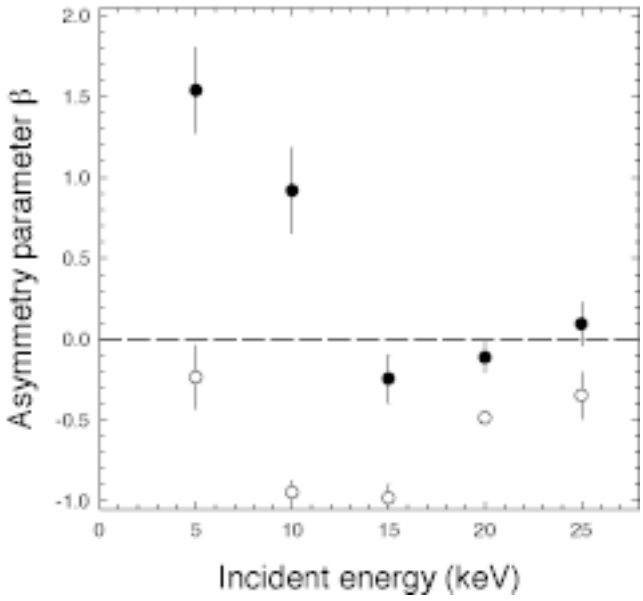

Fig. 4. Asymmetry parameter β versus incident energy for the decay of the $H_2^{+*}(2s\sigma_g, 2p\pi_u)$ molecule in H^+–H_2 collisions: •, present results; ○ Lindsay *et al.* (1987).

and the charge exchange process

$$H^+ + H_2 \longrightarrow H(nl) + H_2^{+*}(2p\sigma_u)\,, \tag{10}$$

while in the present experiment only the charge exchange process (equation 10) leading to $nl = 2p$ was investigated. In light of this, it appears surprising that the two data sets are relatively close to each other and may be an indication that charge exchange and direct ionisation are rather similar processes.

Fig. 4 shows the asymmetry parameter β for the combined $H_2^{+*}(2s\sigma_g)$ and $H_2^{+*}(2p\pi_u)$ channels (equation 3 in connection with equations 4 and 5) as a function of projectile energy. Due to the limited energy resolution of the present experiment it was not possible to separate these two channels. Once again, the measured β is positive and close to $+1{\cdot}5$ at low incident energies, becoming negative around 15 keV and approaching zero around 20–25 keV. Also shown are the results of Lindsay *et al.* (1978), which we obtained by taking a weighted average of their individual β parameters for the $H_2^{+*}(2s\sigma)$ and $H_2^{+*}(2p\pi)$ channels. These data differ significantly from the present ones. One reason for this difference may found in the different weights which the two measurements nevertheless put on the $H_2^{+*}(2s\sigma)$ and $H_2^{+*}(2p\pi)$ channels and, in particular, on the charge exchange channel.

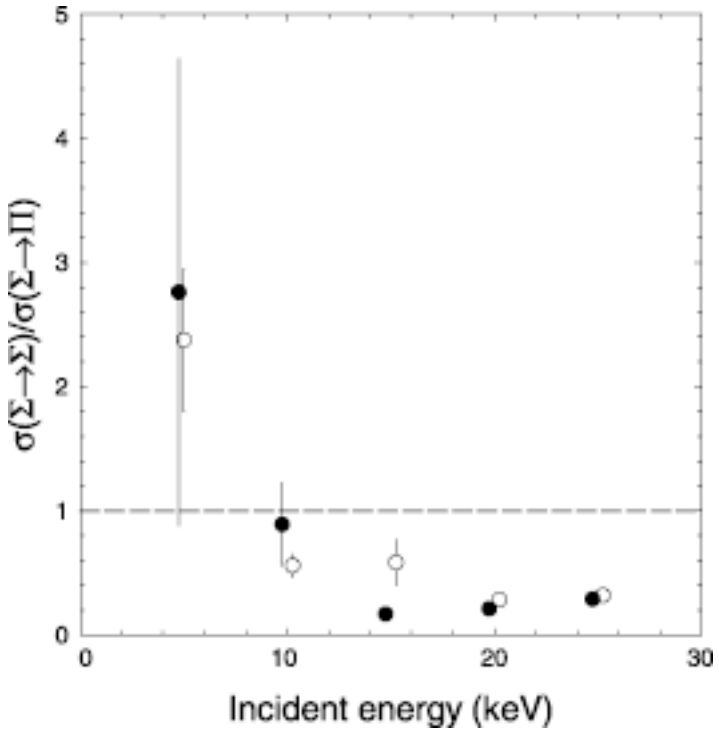

Fig. 5. Relative strength of $\Sigma \rightarrow \Sigma$ compared to $\Sigma \rightarrow \Pi$ transitions versus incident energy for the formation of (○) $H_2^{+*}(2s\sigma_g, 2p\pi_u)$ and (●) $H_2^{+*}(2p\sigma_u)$ molecular ions during H^+–H_2 collisions. For clarity, the data points are displaced by $0{\cdot}25$ keV on the horizontal axis.

In Fig. 5. the relative ratio of $\Sigma \rightarrow \Sigma$ to $\Sigma \rightarrow \Pi$ transitions is displayed. While at 5 keV $\Sigma \rightarrow \Sigma$ transitions seem to be more pronounced, $\Sigma \rightarrow \Pi$ become dominant from 10–25 keV. This result agrees reasonably with polarisation measurements of Lyman-α radiation in H^+–H_2 collisions (Dowek *et al*. 1992), but disagrees with expectations that rotational $\Sigma \rightarrow \Pi$ couplings should dominate at low incident energies. Apparently, the two-electron (ionisation plus excitation) transitions investigated here are more complicated than corresponding one-electron processes in other one- and two-electron systems (Hippler *et al*. 1987, 1988).

Acknowledgments

The authors like to thank Professor Dr H. O. Lutz (Bielefeld) for helpful discussions. This work was supported by the Deutsche Forschungsgemeinschaft in Sonderforschungsbereich 216 'Polarisation und Korrelation in atomaren Stoßkomplexen'.

References

Crowe, A., and McConkey, J. W. (1973). *Phys. Rev. Lett.* **31**, 192.
Dehmer, J., and Dill, D. (1978). *Phys. Rev.* A **18**, 164.
Dowek, D., Tepehan, G., Madeheim, H., and Hippler, R. (1992). *Z. Phys.* D **22**, 735.
Dunn, G., and Kiefer, L. (1963). *Phys. Rev.* **132**, 2109.
Hippler, R., Faust, M., Wolf, R., Kleinpoppen, H., and Lutz, H. O. (1987). *Phys. Rev.* A **36**, 4644.
Hippler, R., Madeheim, H., Harbich, W., Kleinpoppen, H., and Lutz, H. O. (1988). *Phys. Rev.* A **38**, 1662.
Lindsay, B. G., Yousif, F. B., Simpson, F. R., and Latimer, C. J. (1987). *J. Phys.* B **20**, 2157.
Yousif, F. B., Lindsay, B. G., and Latimer, C. J. (1988). *J. Phys.* B **21**, 4157.

Manuscript received 18 February, accepted 11 May 1999